Application of Extracorporeal Shock Wave Lithotripter (ECSWL) in Orthopedics. I. Foundations and Overview

S. H. Park, J. B. Park, J. N. Weinstein,* and S. Loening†

Department of Biomedical Engineering, College of Engineering, *Department of Orthopedics, and †Department of Urology, College of Medicine, The University of Iowa, Iowa City, Iowa

In this paper we have reviewed the feasibility of using a shock wave lithotripter to loosen the interface between the bone and acrylic bone cement for revision arthroplasty. We have reviewed the physics of shock wave and its applications in medicine, especially its interaction with tissues. The calculations show that the energy is greatly reduced at the interface both in the soft tissue–bone interface and cement–bone interface. On the other hand, a tensile and compressive pressure can be operated at the cement–bone interface that can cause the interface to break if the pressure exceeds the tensile strength of the cement–bone interface.

Subsequent papers will deal with *in vitro* and *in vivo* application of the shock wave in the treatment of the cement–bone interface in order to weaken it and consequently for easier extraction of bone cement from the intramedullary canal.

INTRODUCTION

In 1958 Charnley first introduced a self-curing polymethylmethacrylate (PMMA) to orthopedic surgery. Total hip arthroplasty using a PMMA bone cement has dominated orthopaedic surgery for the past three decades. It is estimated to be at 100,000 operations in the United States annually.[1,2] As a result of the number of hip replacements being done, there is a growing number of patients requiring revision arthroplasties. The demand for the hip arthroplasty is continually unabated, and with a population that has an increasing proportion of older people it will increase further. The low complication rate encourages the surgeon to extend the hip arthroplasty to younger patients. But more arthroplasty and a proportionate increase in the number of the late complications are expected. Although improvement in the design and surgical technique will reduce the incidence of the complication in the future, the expected number of failures will be boosted by poor earlier surgical techniques and design of the prosthesis. Therefore, revision hip arthroplasty will dominate in the years to come. According to projections derived from a mathematical model based on 10 years' experience, the ratio of arthroplasty to revision arthroplasty will fall from 4:1 in the year 1982 to 2:1 in the year 1990.[3]

Parts of this paper were presented at the Society for Biomaterials and Orthopedic Research Society Annual meetings.

Requests for reprints should be sent to Dr. Joon B. Park, Department of Biomedical Engineering, College of Engineering, College of Medicine, University of Iowa, Iowa City, IA 52242.

Journal of Applied Biomaterials, Vol. 2, 115–126 (1991)
 CCC 1045-4861/91/020115-12$4.00

The reason for failure of hip arthroplasty includes: femoral component loosening, recurrent dislocation, femoral bone shaft fracture by infection, femoral stem failure and acetabular cup loosening.[4] Acetabular cup loosening was the principle factor of revision arthroplasty.[5] The failure rate of the hip arthroplasty was 5.3% (Charnley–Mueller prostheses, average 5.4 years[5]). The 5.3% failure rate falls within the average range of other long-term studies as given in Table I.[6–20]

An extremely challenging aspect of the revision arthroplasty is the removal of the adherent bone cement from the intramedullary canal which is difficult to reach with instruments.[21,22] One approach to this problem involves the use of osteotomes or power tools to simply drill and chip the cement out from around the femoral stem. Another approach involves cutting a window or a gutter in the cortical bone below the distal end of the femoral stem from the proximal end using special slap hammer extractors, cutting tools, air turbine drills, and fiberoptic headlights.[21–23] Lasers have also been tried recently in an attempt to burn the bone cement out.[25] The drawback of all these new methods and materials is that they are all potentially dangerous to the patient and have not improved a great deal than patients treated with the older procedures.[21,26]

Unfortunately, numerous intraoperative complications have occurred, such as perforation of the femoral cortex by the drilling instruments due to difficulties in differentiating between the hard, brittle cement and adjacent cortical bone, particularly in the intramedullary canal at the level of the isthmus, where blind drilling becomes hazardous. Early studies have reported a 12% rate of intraoperative complications, including femoral shaft fracture during cement removal, femoral shaft perforation, and severe hypotensive crisis secondary to increasing

TABLE I. Long-Term Failure Rate for Total Hip Arthroplasty (Modified Largely from Eftekhar[5])

Authors	Ref. No.	Pub. Year	No. of Hips	Follow-up Years	Failure Rate (%)		
					Mechanical	Infection	Total
Brady & McCretchen	6	1986	170	10–12	8.8	1.4	10.2
Charnley	7	1972	210	4–5	1.3	5.1	6.4
Charnley	8	1979	171	12–15	1.5	3.5	5.0
Charnley & Cupic	9	1973	106	9–10	2.0	4.3	6.3
Collis	10	1977	200	4–6.7	2.0	n/a	2.0
Dall	11	1986	98	12	18.4	2.0	20.4
Eftekhar	12	1971	138	7–8	1.4	3.6	5.0
Eftekhar & Tzitzikalakis	13	1986	699	5–15	3.8	0.7	4.5
Griffith	14	1978	549	7–9	0.9	2.2	3.1
Hamilton	15	1986	450	3–11	0.7	1.6	2.3
Rottger & Elson	16	1986	1971	9–12	9.5	6.9	15.4
Older	17	1986	153	10–12	5.2	0.7	6.0
Salvati	18	1981	67	10	11.7	2.9	14.6
Stauffer	19	1982	207	10	30.5	2.2	32.7
Terayama	20	1986	118	5–12	4.1	1.6	5.7
Total			5453	Average	6.8	2.7	9.5

length of the operation and heavy blood loss.[1,26–30] Furthermore, revision surgery is often performed on elderly patients who are more susceptible to disease.[31] Inadvertent perforation of the femoral shaft occurred in 14% of the revision cases during cement removal from the intramedullary canal. Early studies of revision of total hip arthroplasty showed mortality rate of 3%, which is surprisingly low after more than one major surgical procedure in elderly patients.[29] A more recent report on long-term (average 10.4 years) results of hip arthroplasty for failure of previous surgery indicates 20% of cases required further revision, over half of them for deep infection.[23] They also estimated from the radiographic appearances that eventual failure by loosening will be 58% on femoral side and 56% on the acetabulum side. Others also have reported that the revision arthroplasty would have a higher incidence of morbidity and mortality than the primary procedures.[1,23,26–28]

There continues to be a persistent need for research and innovation to identify a more efficient method of facilitating cement removal. However, recent advances in materials, techniques, and instrumentation have not demonstrated a significant improvement in more recently treated patients who have had revision arthroplasties.

It is hypothesized that loosening the cement–bone interface without adverse effect on the surrounding tissues may facilitate extraction, and the incidence of complications may be decreased by shortening the actual operation time and reducing trauma to the bone. This can be achieved by using the shock wave. Extracorporeal shock wave lithotripsy (ECSWL) is a new technique presently being used to pulverize renal stones by means of repetitive shock waves delivered to a discrete area. This technique, which applies the shock waves to the interface between the bone and the bone cement may be effective in disrupting the cement–bone interface prior to revision surgery to facilitate cement removal.[16]

The ECSWL is a relatively new machine in the United States (FDA approved marketing in December 1984 to the Dornier Medical Systems, Inc., Marietta, GA), which was introduced in Europe in 1976 for breaking up renal calculi without surgery[34–39] and recently for breaking gallbladder stones.[40,41] The Dornier ECSWL machine, a high-voltage underwater spark discharge within an ellipsoid reflector, generates a shock wave which can be focused and transmitted through water. The high-energy wave travels at sonic speed through body tissue, which has similar acoustic impedance with water, with small absorption of energy. At its focal point, the shock wave transforms into mechanical stress against the stone. If the stress overcomes the strength of the calculus then it causes distintegration of the calculus.

The wave from the lithotripter is focused to achieve maximum pressure amplitude at the focal point, while at areas away from it the pressure is reduced, thus decreasing the amount of tissue damage.[36,42,43] Therefore, it is reasonable to summarize the use of the shock wave as based on the following properties[42,43]:

1. Shock waves can generate mechanical stress in solids (such as kidney stone) which could exceed the fracture strength of the material.
2. Shock waves can be transmitted through body tissues without much energy loss if an appropriate transmission medium (e.g., water) is present.

3. Shock waves cause minimal damages to tissues with similar acoustic impedances when transmitted in the body.
4. Shock waves can be focused with suitable wave deflectors and the actual techniques of producing and focusing the shock waves have been well established.

Based on these observations, we have studied the effect of shock waves on the interfacial strength of bone and bone cement in order to facilitate the extraction of the bone cement from the distal portion of intramedullary canal because it is not easily accessible to ordinary instruments and tools.

OVERVIEW OF WAVE PHYSICS

Wave Velocity, Intensity, and Absorption

Waves are divided into two basic types: longitudinal and transverse. Longitudinal waves are those for which motion of particles is along the direction of propagation of the energy. That is, molecules vibrate back and forth in the same direction in which the wave is traveling. Sound waves are longitudinal. The vibration causes local increases and decreases in pressure. These pressure increases and decreases are called compression and rarefaction, respectively. The compression and rarefaction can also be described by density changes and by displacement of the atoms and molecules from their equilibrium positions.

The velocity of sound in a medium is inversely related to the density of the medium. The compressibility of the medium also affects the velocity in an inverse manner. Therefore, velocity of sound waves is described[44,45] as

$$v = \sqrt{\frac{B}{\rho}} \tag{1}$$

where v = wave velocity, ρ = density of the medium, B = bulk modulus of elasticity.

Energy is transmitted by the wave as potential and kinetic energy. The intensity I, energy crossing a unit area per unit time, of a sound wave is given by[44,45]

$$I = \frac{1}{2}\rho v A^2(2\pi f)^2 \tag{2}$$

or

$$I = \frac{1}{2}Z(A\omega)^2 \tag{3}$$

where f = frequency, ω = angular frequency, A = maximum displacement amplitude of atoms or molecules, $Z = \rho v$. The Z, which equals density times wave velocity in a medium, is the acoustic impedance. Some typical values of ρ, v, and Z, which are related for this study, are given in Table II. The intensity can also be expressed as

$$I = \frac{P_0^2}{2Z} \tag{4}$$

where P_0 is the maximum change in pressure. Equation 4 indicates that if two different media have the same intensity value, higher pressure amplitude is reflected by a large value of acoustic impedance.[46,47]

Reflection and Absorption

When a sound wave enters a different medium, part of the wave is reflected and part of the wave is transmitted into the other medium. The ratio of the reflection coefficient R_p and transmission coefficient T_p at the boundary between two media of impedance Z_1 and Z_2 are expressed[44,45]:

$$R_p = \frac{P_r}{P_i} = \frac{Z_2 - Z_1}{Z_2 + Z_1} \tag{5}$$

$$T_p = \frac{P_t}{P_i} = \frac{2Z_2}{Z_2 + Z_1} \tag{6}$$

TABLE II. Acoustic Impedences of Various Materials (Modified from Rose and Goldberg[48])

Materials	Density (kg/m^3)	Velocity (m/s)	Acoustic Impedance ($kg/m^2/s$)
Air	1.2	330	0.004×10^6
Water (20°C)	1000	1437	1.44×10^6
Fat	952	1459	1.39×10^6
Muscle	1080	1580	1.71×10^6
Soft Tissue (ave)	1060	1540	1.63×10^6
Cortical Bone	1763	3333[d]	5.88×10^6
Cancellous Bone	1200[a]	1450	1.74×10^6
PMMA[b]	1180	2670	3.15×10^6
UHMWPE[c]	960	2000	1.92×10^6
Ti6A14V Alloy	4490	4955	22.25×10^6
Stainless Steel	8950	5800	51.91×10^6
Barium Titanate	5400	4460	24.08×10^6

[a]Approximate value.
[b]Polymethylmethacrylate.
[c]Ultra-high molecular weight polyethylene.
[d]Pelker and Saha.[49]

where P_i, P_r, and P_t are, respectively, the pressure amplitudes of the incidence, reflected, and transmitted waves. Reflection at an interface presenting a decrease in impedance to the incoming wave will lead to a phase change in the reflected component. By contrast, the acoustic pressure of a transmitted wave always be in phase, at a boundary, with the incident wave. The energy balance must be maintained at the boundary between the media, the sum of the absolute value of the intensity of the transmitted and reflected wave must be equal to the intensity of the incident wave provided a negligible energy loss at the interface. The corresponding expressions for intensity reflectivity R_i and transmissivity T_i can be given as follows:

$$R_i = \frac{I_r}{I_i} = \frac{(Z_2 - Z_1)^2}{(Z_2 + Z_1)^2} \tag{7}$$

$$T_i = \frac{I_t}{I_i} = \frac{4Z_1Z_2}{(Z_2 + Z_1)^2} \tag{8}$$

From Eqs. 6 and 8, it will be noticed that when a wave propagates from low impedance to high impedance of medium ($Z_1 < Z_2$), such as from soft tissue to bone, the pressure amplitude of transmitted wave is *greater* than that of the incident wave but the transmitted wave energy is *smaller* than that of the incident wave.

When the sound wave passes through medium, there is some energy loss due to frictional effect. The absorption of the energy in the medium causes a reduction in the pressure amplitude and intensity of the sound wave. The pressure amplitude P at a depth x (cm) in a medium is related to the initial pressure amplitude P_0 ($x = 0$) by the exponential equation

$$P = P_0 \exp(-\alpha x) \tag{9}$$

where α, in cm^{-1}, is the absorption coefficient for the medium at a particular frequency. Since the intensity is proportional to the square of the amplitude, Eq. 9, its dependence with depth is

$$I = I_0 \exp(-2\alpha x) \tag{10}$$

where I_0 is the incident intensity at $x = 0$ and I is the intensity at a depth x in the medium. Since the absorption coefficient in Eq. 10 is 2α, the intensity decreases twice rapidly than the amplitude with depth.[44–47]

The absorption coefficient of a wave is related to a frequency of the wave and a viscosity of the medium.[44,45,47] The absorption coefficient of a wave in a biological medium can be expressed by

$$\alpha = bf^m \tag{11}$$

where b, and m are constants, f is frequency of the wave.[30] Most of the biological tissues exhibit a value of the m between 1 and 2. Therefore, high-frequency wave tends to be absorbed more than a low frequency wave.

The half-value thickness is the medium thickness needed to decrease P_0 to $P_0/2$. Because the absorption coefficient differs with the frequency, the half-value thickness also depends on the frequency. Some typical values of absorption coefficients and half-value thickness of ultrasounds are given in Table III.

NATURE OF SHOCK WAVE

Shock Wave Generation

The shock wave used in this study for ECSWL is created by an underwater spark. The spark is generated by a sudden discharge of electrical energy through an appropriate electric circuit that contains an electrode gap submerged in water. The electrical discharge caused by the passage of high voltage across an electrode gap builds up a conductive plasma and causes a dielectric breakdown of water. These sudden changes produce expanding cavitation bubbles. The rapid expansion of this plasma creates an explosive shock, which travels supersonically, and transmits very high pressure to the water. The pressure rise of the shock wave reaches a peak of 100 MPa in approximately 40 nanoseconds.[36] The initial shock wave is transmitted radially. The wave front becomes spherical and decays owing to geometrical divergence and frictional losses to the transporting medium. The electrode is centered in the focal point (F_1) of a metallic ellipsoid reflector. The geometric properties of the ellipsoid are such that the wave is reflected and concentrated to a second focal point (F_2) as shown in Figure 1.

TABLE III. Pressure Absorption Coefficient and Pressure Half-Value Thickness for Various Materials (Modified from Cameron and Skofronick[44])

Materials	Frequency (MHz)	α (cm^{-1})	Half-Value Thickness (cm)
Muscle	1	0.13	5.40
Fat	0.8	0.05	13.45
Bone			
Human Skull	0.6	0.4	1.90
	0.8	0.9	0.68
	1.2	1.7	0.42
	1.6	3.2	0.22
	1.8	4.2	0.16
	3.5	7.8	0.10
Canine Tibia[a]	3	1.4	0.50
	5	2.2	0.32
Human Femur[b]			
Longitudinal	5	2.3	0.30
Radial	5	5	0.14
PMMA[c]	1	0.18	3.88
Water	1	2.5×10^{-4}	2.8×10^3

[a]Alder and Cook.[50]
[b]Lakes et al.[51]
[c]Pearson.[52]

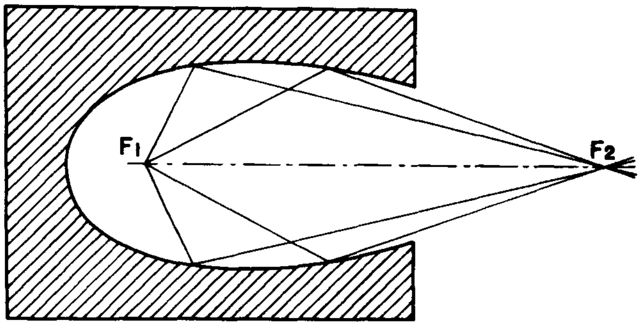

Figure 1. Schematic diagram of wave propagation in ellipsoid reflector and two focal points. An electrode is located at the F_1 position.

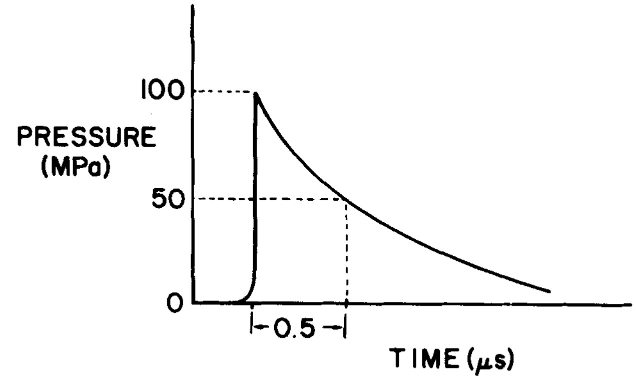

Figure 2. Schematic diagram of shock wave generated by the underwater electrohydraulic spark discharge.

Shock Wave Propagation

Qualitatively, the velocity of all compressive waves, including sound, ultrasound, and shock waves, increases as the compressibility of the transmission medium decreases. In the case of ultrasound, the pressure and the density of the medium remains nearly constant throughout the process of wave transmission. Therefore, all parts of the wave are transmitted at the same velocity so that a wave remains sinusoidal indefinitely during its propagation. But, shock waves cause the transmission medium to become more dense, thus decreasing its compressibility and increasing the wave's velocity.

Initial shock wave, which is an intense sinusoidal half-wave, is created by the bubble expansion as mentioned earlier. At the beginning of the wave, the water is in the low-amplitude range of pressure and therefore the velocity near this area is that of sound. Toward the middle of the wave, the pressure amplitude of each successive point becomes greater, which increases the density of the medium and also the velocity. With continued propagation of the wave, the pressure peak gradually increases its speed enough to overtake the front end of the wave, thus altering its shape. Eventually, spherical shape of the wave transformed into a saw-tooth shape with sharp increase in amplitude pressure followed by a gradual decay of pressure. This results in the typical profile of the shock wave as shown in Figure 2. Once formed, this typical wave form does not propagate indefinitely through a medium without undergoing gradual energy loss.[29,53,54]

Initially, the shock wave has a very sharp rise in pressure at its front, but as transmission continues, energy losses of the high-frequency part reduce this peak pressure until the shock wave degenerates into a sinusoidal wave. In addition to this gradual energy loss, there are secondary tensile or rarefaction waves present that can overtake the main compressive wave and also reduce its peak pressure. This progress is faster in the high viscous medium, such as bone, due to the large energy loss.[53,55]

Unlike ultrasound, shock waves are composed of several different frequency components and have a spectrum.[56] Usually, higher frequencies compose the sharp portion of the wave front and lower frequencies contribute to the shape of the remainder of the wave form. The higher frequency parts of the wave have much more effective energy loss than that of the low-frequency wave (Eq. 11). Shock wave has lower frequency and significantly lower damping capability compared with the ultrasound. Therefore, shock wave has a higher power of penetration than that of the ultrasound.

Pressure Distribution of Shock Wave in Water Medium

Pressure induced by shock wave is usually measured by a pressure transducer. In order to measure a real value of the shock pressure, the pressure transducer must have shorter relaxation time than the duration of the shock wave. Finding a sensitive pressure transducer with a rapid enough response time to accurately record a nanosecond pressure impulse and absolute peak pressure is a problem.[53] Therefore, the absolute values for the shock wave pressure have not yet been reported for the Dornier electrohydraulic lithotripter machine.

Heine[56] measured the shock pressure of the Dornier experimental lithotripter with polyvinylidendifluoride hydrophone. He reported that the sharp peak pressure amplitude was reached about 125 MPa at the second focal point. The pressure curve had a sharp compression wave, with 1 μs of decay, and negligible tensile tailing wave for 80 μs. The peak pressure was found at the second focal point and the pressure was decreased sharply as the distance from the focus was increased. The high pressure was more distributed at the back of F_2 than at the front.

Chaussy[35] reported that the pressure amplitude of the shock wave was increased with widening the electrode separation or increasing the condenser discharge voltage. The maximum pressure amplitude at the second focal point was 150 MPa with the condenser discharge voltage of 27 kV.

The pressure measurement of the clinical ECSWL unit (Dornier HM-3) was done by Hunter and his colleagues by using pizoelectric crystal pressure transducers.[43] The relationship between generator voltage (kV) and peak shock-wave pressure was

$$P_{\text{psi}} = 0.347\ (\text{kV}) + 0.669 \qquad (r^2 = 0.664) \tag{12}$$

which is equivalent to

$$P_{\text{MPa}} = 2.393\ (\text{kV}) + 4.61 \tag{13}$$

The pressure reached up to 62 MPa with 24 kV of generator voltage. The horizontal pressure decreased sharply as the distance from the focus axis was increased. The pressure fell to less than 20% of the highest pressure 1 to 1.5 cm from the focus axis. High pressure was distributed more in axial direction that the horizontal direction.

Pressure Absorption from Second Medium

It is impossible to avoid the transmission of the shock wave through the tissue in the clinical situation. The shock pressure amplitude is reduced when it travels through the tissue. Chaussy[43] studied damping effect of a shock wave with interposing soft tissue. The shock-wave pressure amplitude was decreased 10 to 20% and the half width of the pressure was increased from 18 to 19 mm at the horizontal focal plane after traveled through the 6 cm muscle tissue. But, the location of the second focal point was not changed by the soft tissue. With the 20% reduction of pressure amplitude with 6 cm thickness of muscle tissue, pressure absorption coefficient and half-value thickness can be calculated by using Eq. 9. The calculated values of the absorption coefficient and the half-value thickness are 3.71×10^{-3}/cm and 18.64 cm, respectively. The shock wave pressure in the muscle is, therefore

$$P = P_0 \exp(-3.71 \times 10^{-3} \times 2x) \tag{14}$$

where x is the distance. The pressure half-value thickness of the shock wave in muscle is about 3.5 times thicker than that of 1 MHz ultrasound. Shock wave, having lower frequency, has significantly higher penetration ability compared with the ultrasound.

In order to simulate the shock wave focusing in the tissue, Kuwahara and Takayama[57] measured pressure with 35-mm thick silicone-rubber-covered pressure transducer. The peak pressure was decreased about 50% and the pressure profile was widened over the focal point.

SHOCK WAVE AND TISSUE INTERACTIONS

Effect on Soft Tissue

There have been many reports on the soft tissue damages by shock wave. Tissue damages are liable to occur in the focus of shock wave. Lung tissue is particularly vulnerable due to the low acoustic impedance.[58–60] In animal experiments, several types of tissue damage after shock-wave exposure have been reported, including cutaneous petechiae, subcutaneous, and muscle hematoma at the shock wave entry, interstitial edema, petechial bleeding, intraparenchymal and subcapsular hematomas, transient macrohematuria, and temporary loss of kidney function.[59–61] The mechanism of trauma to tissue is unknown. The primary factors associated with these impairments include the maximum pressure itself, the preceding shock wave, the following tensile wave, and the effects of cavitation bubbles.[61,62]

Effect on Hard Tissue

The effect of shock wave on the hard tissues has not been studied extensively. Due to the high percentage of the collagen matrix and crystalline composition, bone may not appear to be affected by shock wave. Eisenberger and co-workers[63] applied double shock wave with a power of 25 kV to freshly removed human bone tissues (femur, rib, vertebral body, and sternum). The test specimen was freely suspended at the focal point. The femur was fractured with single shock-wave exposure. But, double shocks produced no visible and histological changes in the rib, vertebra, or sternum.

Yeaman and co-worker[64] applied 1500 shock waves at 20 kV to a proximal tibia of 5-week-old rat with the Dornier experimental XL-1 lithotripter. Two, four, and ten weeks later, they were sacrificed. Lesions of focal growth plate dysplasis was found at the treated tibia, but no other major damage was observed. Most of the lesion was resorbed in 4 weeks and completely replaced with new bone in 10 weeks.

Karpman[65] treated a bone cement implanted cadaveric canine femur with shock waves. One hundred shock impulses were targeted at the cement–bone interface. Some microfractures were found at the cortical bone that contacted with the bone cement, but no major damage on the bone was found.

SHOCK WAVE EFFECT ON THE CEMENT–BONE INTERFACE

Strength of Interface

There is no chemical bonding between bone and cement.[66] The only source of the interfacial strength of bone and cement is the mechanical retention of the bone cement due to interdigitation with bone. Therefore, cement–bone interface is the weakest link in the implant fixation system. Cement–bone interfacial strength is generally related to the surface topology of interdigitation. The amount and shape of porosity in cancellous bone would affect the total cement–bone interfacial volume. Increased cement intrusion to cancellous bone provides the greater interfacial strength. The cleanness and the dryness of bone during the cement insertion also greatly affect the interfacial strength. Tensile strength of the cancellous cement–bone interface is approximately 2.7 MPa.[67]

The cement–bone interface is often changed due to bone remodeling and fibrous membrane generation. Direct cement–bone contact is disconnected by the fibrous layer. The thickness of the fibrous membrane varied from few μm to around 1 mm. This type of interface is primarily suitable for transmitting compressive stress but with almost no ability to transmit tensile stress.[68,69]

Shock Wave Profile in Bone and Cement

In order to break a cement–bone interface with shock wave, the shock wave has to travel through the soft tissue, bone, and bone cement. The acoustic impedances of the soft tissue, bone, and cement are, respectively, 1.63, 5.88, and 3.15×10^6 kg m^{-2} s^{-1}. Due to the acoustic impedance change of the medium, the shape of the shock wave is changed during the propagation. If the target point of the shock wave is located at the cement–bone interface, the shock wave accumulates and alters its shape to a sudden discontinuous sharp peak until it reaches to the muscle–bone boundary. At the muscle–bone boundary, the wave reflection and transmission take place. The transmitted wave amplitude becomes higher than that of incident (Eq. 6) but its energy is lower than that of incident (Eq. 8). Due to the higher wave velocity and higher viscosity in the bone medium at the shock front, particle velocity cannot overtake the wave velocity any more.[53,55] Eventually, the wave loses its sharpness. As transmission continues, the energy loss reduces its peak pressure and the wave shape becomes more spherical. The attenuation of the wave in the bone is due to the several factors; viscoelastic loss associated with the collagenous phase of bone, losses from fluid flow, and conversion of energy into slow wave motion.[51,70] At the cement–bone boundary, another-reflection and transmission of wave take place. Not like at the muscle–bone boundary, the transmitted wave amplitude and energy become lower than those of the incident (Eqs. 6 and 8). The transmitted wave loses more energy and its shape degenerates to a sinusoidal wave. The reflected wave changes its phase to a tensile wave at the boundary.

Prediction of Pressure and Energy in Bone and Cement

If the shock wave obeys the acoustical laws linearly, shock pressure and energy in the bone and cement can be predicted by using Eqs. 5 through 8. The calculation was based on the following assumption: Due to no reported absorption coefficient of the shock wave in the muscle and bone, the absorption coefficient of the femur was figured out from the reported ultrasound absorption coefficients and half-value thickness[44,51] and Chaussy's[35] experiment. From Chaussy's experiment, half-value thickness of the shock wave was 3.5 times larger than that of 1 MHz ultrasound. If we assume that the half-value thickness has a linear relationship between the ultrasound and the shock wave, the half-value thickness of the shock wave in radial direction of femur, which is shorter than that of longitudinal direction, becomes 0.49 cm, which is 3.5 times thicker than that of ultrasound. Using Eq. 9, the absorption coefficient of the shock wave in the radial direction of the bone was obtained as 1.41 cm^{-1}. The thickness of the bone was also assumed as 0.6 cm for the calculation of the energy and pressure absorption in the bone. The calculated wave pressure and energy transfer at the boundaries are given in Table IV and illustrated in Figure 3.

When 100% of the pressure and energy enter the soft tissue–bone interface, 32.0% of the energy is reflected and 68.0% of the energy is transmitted. The transmitted and reflected pressure become 156.5% and 56.5%, respectively, of the incident pressure. The wave undergoes attenuation in the bone. Because pressure and energy loss in the bone are 57.3% and 81.7%, respectively, only 67.0% of the initial pressure and 12.4% of the initial energy are reached at the cement–bone boundary. At the second boundary, 70.6% of the pressure and 91.3% of

TABLE IV. Pressure and Energy Transfer in Soft Tissue–Bone and Cement–Bone Boundary

	Soft Tissue–Bone Boundary			Cement–Bone Boundary	
	Reflect.	Trans.	Bone[a]	Reflect.	Trans.
Pressure	0.565	1.565		−0.294	0.706
Absorption	—	—	57.3%	—	—
% of Incident Pressure[a]	56.5%	156.5%		−19.7%	47.3%
Energy	0.320	0.680		0.087	0.913
Absorption	—	—	81.7%	—	—
% of Incident Energy[b]	32.0%	68.0%		1.0%	11.4%

[a] $\alpha = 1.41\,\mathrm{cm}^{-1}$, 0.6 cm in thickness.
[b] Incident pressure of energy is 100.
$Z_{\mathrm{s.\ tissue}} = 1.63$, $Z_{\mathrm{bone}} = 5.87$, $Z_{\mathrm{cement}} = 3.20$ (kg m^{-2} s^{-1}).

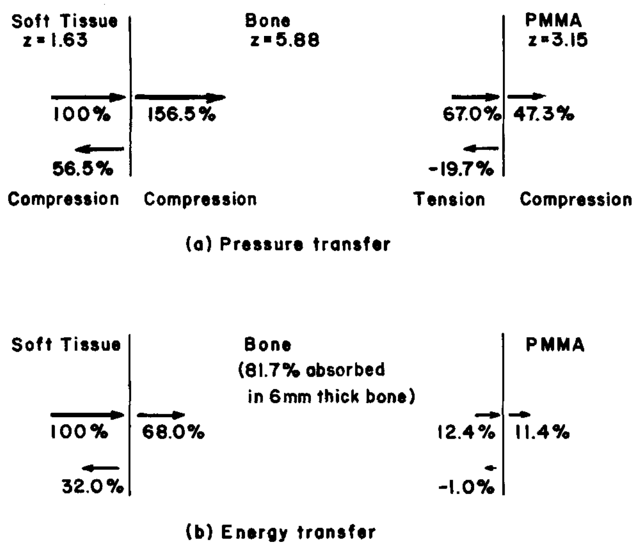

Figure 3. Shock-wave transfer in soft tissue, bone, and cement.

the energy are transmitted to the cement and 29.4% of the pressure and 8.7% of the energy are reflected. Therefore, 47.3% of the initial pressure and only 11.4% of the initial energy are transmitted to the cement. Also, 19.7%, whose phase is changed, of the initial pressure reflected to the bone. If 20 kV of the discharge voltage generates 120 MPa of pressure at the second focal point, about 10 to 20% of the pressure is absorbed by the muscle.[36] Then, approximately 100 MPa of pressure enters to the bone. The transmitted pressure to the bone becomes 156.5 MPa of compressive stress. This stress is close to the ultimate compressive strength of the bone. Due to the increase of the ultimate compressive or tensile strength with high strain rate, the bone may not be damaged by the pressure. Finally, 19.7 MPa of tensile stress and 47.3 MPa of compressive stress are acting on the bone and bone cement, respectively. These opening stress may break the interdigitation of the bone and cement.

If fibrous membrane is present between bone and cement, smaller amplitude of the pressure and energy are transmitted to the bone cement. It was assumed that there were no energy or pressure absorption in the fibrous layer. The thickness of the fibrous layer is too thin to compare with the half-value thickness of the soft tissue. However, the reflected pressure amplitude to the bone is slightly higher than that from the cement–bone boundary. Because acoustic impedance of the fibrous layer is lower than that of the cement, more pressure is reflected. Table V and Figure 4 show the calculated pressure and energy transfer at the fibrous layer.

Mechanism of Cement–Bone Interface Loosening

Hopkinson's pressure bar, which was first developed in late 1800s by Betram Hopkinson,[71] can explain the breaking mechanism of cement–bone interface more practically. The Hopkinson's pressure bar is illustrated in Figure 5. A transient impact from an explosive is applied to the end A of the bar AB. A short piece C of the same material and diameter as the bar is affixed to the other end of the bar with a glue. The pressure wave passes through the junction at B with little modification, but the reflected rarefaction interacting with the tail of the pressure pulse produces a tension at B. The piece then flies off the end, trapping some of the momentum of the incident wave. Similar phenomenon may happen at the cement–bone interface when the shock wave is applied.

Actually, the cement–bone interface is not flat and the cement is interdigitated with the bone trabeculae. The breaking mechanism of the interdigitated cement–bone interface can be explained in the following way. The shock waves arrive at the cement–bone interface simultaneously as shown in Figure 6a. Two zones of the bone are under compression. The shock waves at zone 1 undergo transmission and reflection at the boundary while other shock wave is still traveling in the bone (Fig. 6b). Therefore, three zones of the bone are under different pressure, tension in zone 1, compression in zone 3, and shear in zone 2. If these shear stress exceed the shear strength of the trabeculae bone, fracture of the

TABLE V. Pressure and Energy Transfer in Bone–Fibrous Layer and Fibrous Layer–Cement Boundary

	Bone[a]–Fibrous Layer Boundary		Fibrous Layer	Fibrous Layer–Cement Boundary	
	Reflect.	Trans.		Reflect.	Trans.
Pressure	−0.565	0.435		0.325	1.325
Absorption	—	—	0%	—	—
% of Incident Pressure[a]	−37.8%	29.1%		9.5%	38.6%
Energy	0.320	0.680		0.106	0.894
Absorption	—	—	0%	—	—
% of Incident Energy[b]	4.0%	8.4%		0.9%	7.5%

[a]0.6 cm in thickness.
[b]Incident pressure of energy is 100.
$Z_{fiber} = 1.63$, $Z_{bone} = 5.87$, $Z_{cement} = 3.20$ (kg m^{-2} s^{-1}).

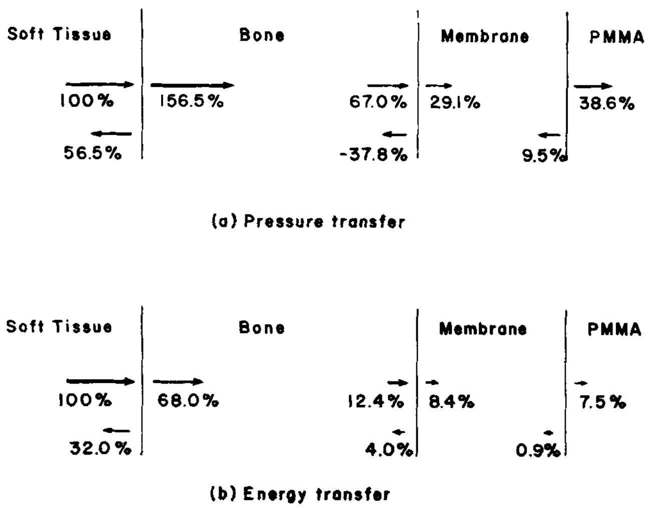

Figure 4. Shock-wave transfer in bone, fibrous membrane, and cement.

trabeculae occurs. If not exceeds, the shear stress weakens the trabeculae. Also, breaking of the cement–bone interface at the zone 1 occurs at this point. As the wave travels more, opposite pressure is applied to the bone and cement. All parts of the cement are under compression except zone 2, and the bone in zone 3 is under tension (Fig. 6c). In this situation, interface of zone 1 is broken. With repeated application of the shock wave, either total breaking of interdigitted cement–bone interface or weakening of the cancellous bone may be achieved (Fig. 6d).

PREVIOUS STUDIES

Clinical Trial Report

Weinstein and co-workers[33] have reported the first trial of the shock wave for the revision of total knee arthroplasty. Two planes on the cement–bone interface around the tibial component were treated with the shock wave. Each plane received 1200 shock impulses of 20 kV of generator voltages with the Dornier HM-3. The post-treatment roentgenograms showed a subtle widening of the tibial lucent line at the cement–bone interface. Five days after the treatment, total revision was performed. The tibial component and all its cement were removed *en bloc* while the femoral component was not loose.

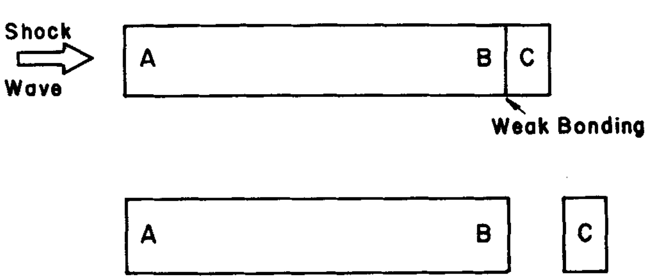

Figure 5. Diagram of Hopkinson's bar.

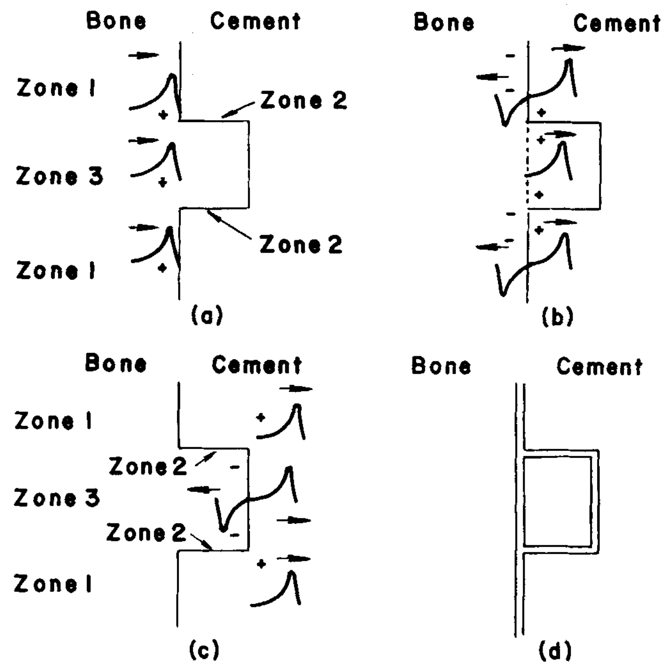

Figure 6. Hypothetical loosening mechanism of interdigitated cement–bone interface.

Loosening of Interface

Karpman and co-workers[65] have examined the shock-wave-treated cement–bone interface microscopically. The acrylic bone cement and a stainless steel rod were implanted in the reamed medullary canal of canine femur. After 24 h, the cement–bone interface was treated with 100 shock waves with the Dornier Lithotripter (power setting of the lithotripter was not reported). They found no radiographical difference between the pre-treated and the posttreated specimens. They also found many microfractures in the bone cement and a definite disturbance of the cement–bone interface with SEM and light microscopic examinations. Some microfractures were also seen in the surrounding cortical bone. There was no overt loosening of the implant upon manual manipulation.

May and co-workers[72] have studied the effect of the shock wave on the cement–bone interfacial shear strength. The bone cement and a threaded stainless steel rod were implanted in the reamed medullary canal of canine femur with a depth of 4 in. Three points with 2-cm intervals were shock-wave treated. The shock wave targeted at the center of the steel rod and each point was exposed to 1000 impulses of 25 kV. After treatment, the steel rod with cement were pulled out at a rate of 1 in./min. The result was that the shock-wave-treated bone cement interfacial shear strength was an average 43.1% lower than that of the untreated.

Other researchers[73] have tried to use the shock wave to loosen the interface between porous implant and bone after 3 months in rabit femur. The pull-out force was decreased by 17.5% after treating 2000 shocks at 26 kV compared with the contralateral controls, but it was not statistically significant ($p = 0.06$).

Effect on Acrylic Bone Cement

May and co-workers[74] also have investigated the effect of the shock wave on the mechanical properties of PMMA bone cement. The prepared tensile and compression test specimens were treated with 1000 impulses of the shock wave with different power setting. After the treatment, compressive strength, tensile strength, and compressive elastic modulus were measured. They reported that there was no significant difference between the untreated and the treated in both the compressive strength and the elastic modulus, up to 25 kV of power level. But, the ultimate tensile strength was decreased 10 to 20% with 25 kV of power setting. Also, fatigue properties were diminished.[74]

DISCUSSION

In this paper we have tried to lay down the fundamental principles of wave physics and their use in loosening the interface between bone and bone cement for revision arthroplasties. Essentially the interface can be disrupted due to the acoustic impedance difference between them. The exact mechanism of the disruption beyond the rough assumption presented in this paper should be explored further.

Our *in vitro* and *in vivo* experimental results as well as dose–response measurements of the shock-wave treatments[75,76] will be presented in subsequent papers. It is hoped that this work will stimulate further studies in this area of vital importance.

This work has been carried out as a part of PhD thesis (SHP). This work was supported in part by the Dornier Medizintechnik, GmbH (Munich, Germany) and Department of Biomedical Engineering, University of Iowa, Iowa City, Iowa.

REFERENCES

1. Pellicci, P.; Wilson, P.; Sledge, C.; Salvati, E.; Panawat, C.; Poss, R. Revision total hip arthroplasty. Clin. Orthop. Rel. Res. 170:34–41; 1982.
2. Huiskes, R. Introduction in some fundamental aspects of human joint. Acta. Orthop. Scand., (Suppl.) 185:1–10; 1980.
3. Morscher, E.; Schmassmann, A. Failures of total hip arthroplasty and probable incidence of revision surgery in the future: calculations according to a mathematical model based on a ten year's experience in total hip arthroplasty. Arch. Orthop. Trauma. Surg. 101:137–143; 1983.
4. Balderstone, R. A. Results of primary total hip replacement. Booth, E. Jr. ed. Total Hip Arthroplasty, Philadelphia: W. B. Saunders Co.; 1988:160–173.
5. Eftekhar, N. S. Long-term results of cemented total hip arthroplasty. Clin. Orthop. Rel. Res. 225:207–217; 1987.
6. Brady, L. P.; McCutchen, J.W. A ten year follow-up study of 170 Charnley total hip arthroplasties. Clin. Orthop. Rel. Res. 211:51–54; 1986.
7. Charnley, J. The long-term results of low-friction arthroplasty of the hip, performed as a primary intervention. J. Bone Joint Surg. 54B:61–76; 1972.
8. Charnley, J. Low friction arthroplasty of the hip, theory and practice, Heidelberg: Springer-Verlag; 1979.
9. Charnley, J.; Cupic, Z. The nine and ten year results of the low-friction arthroplasty of the hip. Clin. Orthop. Rel. Res. 95:9–25; 1973.
10. Collis, D. K. Femoral stem failure in total hip replacement. J. Bone Joint Surg. 59A:1033–1041; 1977.
11. Dall, D. M.; Grobbelaar, C. J.; Learmonth, I. D.; Dall, G. Charnley low-friction arthroplasty of the hip: long term results in South Africa. Clin. Orthop. Rel. Res. 211:85–90; 1986.
12. Eftekhar, N. S. Charnley "low friction torque" arthroplasty. A study of long-term results. Clin. Orthop. Rel. Res. 81:93–105; 1971.
13. Eftekhar, N. S.; Tzitzikalakis, G. Failure and reoperations following low-friction arthroplasty of the hip. Clin. Orthop. Rel. Res. 211:65–78; 1986.
14. Griffith, M. J.; Sedenstein, M. L.; Williams, D.; Charnley, J. Socket wear in Charnley low friction arthroplasty of the hip. Clin. Orthop. Rel. Res. 137:37–47; 1978.
15. Hamilton, H.W.; Joyce, M. Long term results of low friction arthroplasty performed in a community hospital, including a radiologic review. Clin. Orthop. Rel. Res. 211:55–64; 1986.
16. Rottger, J.; Elson, R. A modification of Charnley low-friction arthroplasty, representative ten-year follow-up results of the St. Georg prosthesis. Clin. Orthop. Rel. Res. 211:154–163; 1986.
17. Older, J. Low-friction arthroplasty of the hip. A 10–12 year follow-up study. Clin. Orthop. Rel. Res. 211:36–42; 1986.
18. Salvati, E. A.; Wilson, P. D. Jr.; Jolley, M. N.; Vakili, F.; Aglietti, P.; Brown, G. C. A ten year follow up study of our first one hundred consecutive Charnley total hip replacements. J. Bone Joint Surg. 63A:753–767; 1981.
19. Stauffer, R. N. Ten-year follow-up study of total hip replacement. J. Bone Joint Surg. 64A:983–990; 1982.
20. Terayama, K. Experience with Charnley low-friction arthroplasty in Japan. Clin. Orthop. Rel. Res. 211:79–84; 1986.
21. Harris, W. H.; White, R. E.; Mitchell, S.; Barber, F. A new technique for removal of broken femoral stems in total hip replacement. J. Bone Joint Surg. 63A:843–845; 1981.
22. Mollen, R. A. B.; McClleland, C. J. Instrumentation for the revision of total hip arthroplasty. Clin. Orthop. Rel. Res. 186:16–22; 1986.
23. Harris, W. H.; Oh, I. A new revision tool for removal of methylmethacrylate from the femur. Clin. Orthop. Rel. Res. 132:53–54; 1978.
24. Harris, W. H. Revision surgery for failed, nonseptic total hip arthroplasty, the femoral side. Clin. Orthop. Rel. Res. 170:8–20; 1982.
25. Beacon, J.; Aichroth, P.; Baird, P. The carbon dioxide laser as a surgical tool for the removal of bone cement. Revision Arthroplasty, Proceedings of a Symposium at Sheffield University, Oxford: Oxford Medical Education Service, Ltd; 1979:99.
26. Pellicci, P. M.; Wilson, P. D.; Sledge, C. B.; Salvati, E. A.; Panawat, C. S.; Callaghan, J. J. Long term results of revision total hip replacement. J. Bone Joint. Surg. 67A:513–516; 1985.
27. Amstutz, H.; Markolf, K. L.; McNeice, G. M.; Gruen, T. A. Loosening of total hip components, cause and prevention. The Hip, St. Louis: C.V. Mosby Co.; 1976:102–116.

28. Eftekhar, N.; Smith, E.; Henry, J.; Stinchfield, F. Revision arthroplasty using Charnley low friction arthroplasty technic. Clin. Orthop. Rel. Res. 95:49–59; 1973.
29. Hunter, G. A.; Welsh, R. P.; Cameton, H. U.; Bailey, W. H. The results of revision of total hip arthroplasty. J. Bone Joint. Surg. 61B:419–421; 1979.
30. Khan, M.; O'Driscoll, M. Fractures of femur during total hip replacement and their management. J. Bone Joint Surg. 59B:36–41; 1977.
31. Carmer, S. Surgical complication in revision arthroplasty. Tuner, R. ed. Revision Total Arthroplasty, New York: Grune & Stratton; 1982.
32. Echeverri, A.; Shelley, P.; Wroblewski, B. M. Long-term results of hip arthroplasty for failure of previous surgery. J. Bone Joint. Surg. 70B:49–51; 1988.
33. Weinstein, J. N.; Wroble, R. R.; Loening, S. Revision total joint arthroplasty facilitated by extracorporeal shock wave lithotripsy: a case report. Iowa Orthop. J. 6:121–124; 1986.
34. Brendel, N. Shock waves: a new physical principle in medicine. Eur. Surg. Res. 18:177–180; 1986.
35. Chaussy, C. H. Extracorporeal Shock Wave Lithotripsy, Basel, Munchen: Karger Publishers; 1982.
36. Chaussy, C. H. Extracorporeal Shock Wave Lithotripsy. New Revised Edition, Basel, Munchen: Karger Publishers; 1986.
37. Chaussy, C. H.; Schmiedt, E. Shock wave treatment for stones in the upper urinary tract. Urol. Clin. N. Amer. 10:743–750; 1983.
38. Chaussy, C. H.; Schmiedt, E.; Jocham, D.; Schuller, J.; Brendel, W.; Liedl, B. Extracorporeal shock wave lithotripsy treatment for urolithiasis. Special Issue to Urology 23:59–66; 1984.
39. Drach, G.W.; Dretler, S.; Fair, W.; Finalyson, B.; Gillenmeter, J.; Griffith, D.; Lingeman, J.; Newman, D. Report of the United States cooperative study of extracorporeal shock wave lithotripsy. J. Urol. 135:1127–1133; 1986.
40. Neubrand, M.; Sauerbruch, I.; Stellaard, F.; Paumgartner, G. In vitro cholesterol gallstone dissolution after fragmentation with shock waves. Digestion 34:51–59; 1986.
41. Sauerbruch, T.; Delius, M.; Paaumgartner, G.; Holl, J.; Wees, O.; Weber, W.; Hepp, W.; Brendel, W. Fragmentation of gallstones by extracorporeal shock wave. New Engl. J. Med. 314:818–822; 1986.
42. Chaussy, C. H.; Schmiedt, E.; Jocham, D.; Brendel, W.; Walther, V. First clinical experience with extracorporeally induced destruction of kidney stones by shock waves. J. Urology 127:417–420; 1982.
43. Hunter, P.; Finlayson, B.; Hiroko, R.; Voreck, W.; Walker, R.; Walck, S.; Nasr, M. Measurement of shock wave pressures used for lithotripsy. J. Urol. 136:733–738; 1986.
44. Cameron, J.; Skofronick, J. Sound in Medicine in Medical Physics, New York: Wiley; 1979.
45. Christensen, D. Ultrasonic Bioinstrumentation. New York: Wiley; 1988.
46. Shutlov, V. A. Fundamental Physics of Ultrasound, New York: Gordon Breach Science Publisher; 1988.
47. Bamber, J. Attenuation and absorption. Hill, C. ed. Physical Principles of Medical Ultrasonics, New York: Wiley; 1986:118–199.
48. Rose, J.; Goldberg, B. Ultrasound principles in basic physics. Rose, J. ed. Diagnostic Ultrasound, New York: Wiley; 1979.
49. Pelker, R.; Saha, S. Stress wave propagation in bone. J. Biomechanics 16:481–489; 1983.
50. Aldler, L.; Cook, K. Ultrasonic parameters of freshly frozen dog tibia. J. Acous. Soc. Am. 58:1107–1108; 1975.
51. Lakes, R.; Yoon, H.; Katz, L. Ultrasonic wave propagation and attenuation in wet bone. J. Biomed. Eng. 8:143–148; 1986.
52. Pearson, J. A Theory of Waves, Boston: Allen and Bacon; 1966.
53. Fedoseeva, T.; Fridman, F.; Goldberg, V.; Zarnitsina, I. Relaxation effects in the propagation of underwater shock wave. Lauterborn, W. ed. Cavitation and Inhomogeneities in Under Water Acoustics, New York: Springer-Verlag; 1977.
54. Hunter, P. The physics and geometry pertinent to ESWL. Riehle, R. ed. Principles of Extracorporeal Shock Wave Lithotripsy, New York: Churchill Livingstone; 1987.
55. Nakoryakov, V.; Pokusaev, B.; Shreiber, I. Pressure waves in liquid with gas or vapor bubbles. Lauterborn, W. ed. Cavitation and Inhomogeneities in Under Water Acoustics, New York: Springer-Verlag; 1979.
56. Heine, G. Physical aspects of shock wave treatment. Gravenstein, J. ed. Extracorporeal Shock-Wave Lithotripsy for Renal Stone Disease, Stoneham, MA: Butterworth Publishers; 1986.
57. Kuwahara, M.; Takayama, K. Extracorporeal microexplosive lithotripter. Kandel, L. ed. State of the Art Extracorporeal Shock Wave Lithotripsy, Mount Kisco, NY: Futura Publishing Co, Inc.; 1987.
58. Brendel, W. History of shock-wave treatment of renal concrements. Gravenstein, J. ed. Extracorporeal Shock-Wave Lithotripsy for Renal Stone Disease, Stoneham, MA: Butterworth Publishers; 1986.
59. Newman, D.; Lingeman, J.; Mertz, J.; Mosbaugh, P.; Steele, R.; Knapp, P. Jr. Extracorporeal shock-wave lithotripsy. Urol. Clin. N. Amer. 14:63–71; 1987.
60. Woodruff, R.; Kandel, L. Effect of ESWL on the kidney and adjacent tissue. Kandel, L. ed. State of the Art Extracorporeal Shock Wave Lithotripsy, Mount Kisco, NY: Futura Publishing Company, Inc.; 1987.
61. Fischer, N.; Muller, H.; Gulhan, A.; Sohn, M.; Deutz, F.; Rubben, H.; Lutzeyer, W. Cavitation effects: a possible cause of tissue injury during extracorporeal shock wave lithotripsy. Lingeman, J. ed. Shock Wave Lithotripsy, New York: Plenum Press; 1988.
62. Williams, A.; Delius, M.; Miller, D.; Schwarze, W. Investigation of cavitation in flowing media by lithotripter shock waves both in vitro and in vivo. Ultrasound Med. Biol. 15:53–60; 1989.
63. Eisenberger, F.; Chaussy, C. H.; Wanner, K. Extrakoporale Anwendung von hochenergetichen Stszwellen—Ein Nuer Aspekt in der Behaandlung des Harnsteinleidens. Aktuelle Urologie 8:3–15; 1977.
64. Yeaman, L.; Jerome, C.; MaCullough, D. Effects of shock waves on the structure and growth of the immature rat epiphysis. J. Urol. 141:670–674; 1989.
65. Karpman, R. R.; Magee, F. P.; Gruen, T.W. S.; Mobley, T. The lithotripter and its potential use in the revision of total hip arthroplasty. Orthoped. Rev. 16:38–42; 1987.
66. Park, J. B. Acrylic bone cement: in vitro and in vivo property–structure relationship—a selective review. Ann. Biomed. Eng. 11:297–312; 1983.
67. Krause, W.; Krug, W.; Miller, J. Strength of the cement–bone interface. Clin. Orthop. Rel. Res. 163:290–299; 1982.
68. Radin, E.; Rubin, C.; Thrasher, E.; Lanyon, L.; Clugnola, A. Change in the bone–cement interface after total hip replacement. J. Bone Joint Surg. 64A:1188–1200; 1982.
69. Walker, P. S. ed. Fixation, in Human Joint and Their Artificial Replacements, Springfield, IL: Thomas; 1977.

70. Lakes, R.; Yoon, H.; Katz, L. Slow compressional wave propagation in wet human and bovine cortical bone. Science, 220:513–515; 1983.
71. Duvall, G. E. The physics connection. Murr, L. E. ed. Metallurgical Application of Shock-Wave and High-Strain-Rate Phenomena, New York: Marcel Dekker, Inc.; 1986.
72. May, T.; Krause, W.; Beaudoin, A.; Preslar, A.; Smith, M. The effects of high energy shock waves on the mechanical properties of acrylic bone cement. Seventh Southern Biomedical Engineering Conference Transaction, Oct. 27-28, 1988:113–115.
73. Fyda, T. M.; Stranne, S. K.; Fulghum, C. S.; Glisson, R. R.; Weinerth, J. L.; Seaber, A.V.; Callaghan, J. J. Strength of fixation in porous-coated implants exposed to lithotripsy. To be presented in the 37th Annual Orthop. Res. Soc. Meeting, Anaheim, CA, March 1991.
74. May, T. C.; Krause, W. R.; Smith, M. J.V.; Cardea, J. A.; Davenport, J. M. Fracture and fatigue of lithotripted (ESWL) PMMA bone cement. 16th Ann. Soc. Biomat. Meeting Trans., 106, Charleston, SC, May 1990.
75. Park, J. B.; Park, S. H.; Weinstein, J. N.; Loening, S.; Oster, D. Application of extracorporeal shock wave lithotripter (ECSWL) in orthopedics. II. Dose–Response and Pressure Distribution Measurements, to appear.
76. Weinstein, J. N.; Park, S. H.; Park, J. B.; Loening, S.; Oster, D. Application of extracorporeal shock wave lithotripter (ECSWL) in orthopedics. III. in vitro and in vivo studies, to appear.

Received October 19, 1990
Accepted February 1, 1991